

# Stripes, spin resonance and $d_{x^2-y^2}$ -pairing symmetry in FeSe-based layered superconductors

Tanmoy Das<sup>1</sup>, and A. V. Balatsky<sup>1,2</sup>

<sup>1</sup>*Theoretical Division, Los Alamos National Laboratory, Los Alamos, NM-87545, USA. and*

<sup>2</sup>*Center for Integrated Nanotechnology, Los Alamos National Laboratory, Los Alamos, NM 87545, USA*

(Dated: July 13, 2022)

We calculate RPA-BCS based spin resonance spectra of newly discovered iron-selenide superconductor using two orbitals tight-binding (TB) model. The slightly squarish electron pocket Fermi surfaces (FSs) at  $(\pi, 0)/(0, \pi)$ -momenta produce leading inter-pocket nesting instability at incommensurate vector  $q \sim (\pi, 0.5\pi)$  in the normal state static susceptibility, pinning a strong stripe-like spin-density wave (SDW) or antiferromagnetic (AFM) order at some critical value of  $U$ . The same nesting also induces  $d_{x^2-y^2}$ -pairing. The superconducting (SC) gap is nodeless and isotropic on the FSs as they are concentric to the four-fold symmetry point of the  $d$ -wave gap maxima, in agreement with various measurements. This induces an slightly incommensurate spin resonance with ‘hour-glass’-like dispersion feature, in close agreement with neutron data of chalcogenides. We also calculate  $T$  pendency of the SC gap solving BCS gap equations and find that the spin resonance follows the same  $T$  evolution of  $\Delta(T)$  both in energy and intensity, suggesting that an itinerant weak or intermediate pair coupling theory is relevant in this system.

PACS numbers: 74.70.-b, 74.20.Rp, 74.20.Pq, 74.20.-z

The newly discovered high- $T_c$  superconductor in iron-selenide (FeSe-) based compounds[1], not only increase the number of unconventional SC family, but bears on several unique magnetic and SC properties coming from its unusual FS properties. Both ARPES[2–4] and followed by LDA calculations[5], have demonstrated that the FS is consist of only two electron pockets at  $(\pi, 0)/(0, \pi)$ , while the hole pockets lie below the Fermi level ( $E_F$ ) and do not appear on the FS at the dopings considered experimentally to date. Specific heat[6], and ARPES[2–4] studies find that these FSs are nodeless and isotropic. Evidences are mounting from NMR,[7], Raman,[8],  $\mu$ SR[9], optical[10] and other experiments[11], and supported by LDA calculations[5] that these materials possess magnetic order ground state which coexists with superconductivity.

In cuprates, the FS is a hole-like centering  $(\pi, \pi)$  point and the nesting between inter FS is strongest along  $Q = (\pi, \pi)$  which is responsible for SDW,  $d_{x^2-y^2}$ -wave pairing and a spin resonance peak at  $Q$  with ‘hour-glass’ dispersion in the SC state.[12] In Ce-based heavy fermion, the hole pockets at  $(\pi, \pi)$  lead to  $(\pi, \pi, \pi)$ -resonance with  $d_{x^2-y^2}$ -wave symmetry.[13] In iron-pnictide[14] and iron chalcogenides,[15–18] the FS has two hole-pockets at  $\Gamma$  and two electron-pockets at  $(\pi, 0)/(0, \pi)$  in unfolded one Fe unit cell and the leading nesting between the hole and electron pockets constitute  $(\pi, 0)$ -SDW,  $s^\pm$ -pairing and  $(\pi, \pi)$ -spin resonance with a ‘hour-glass’ dispersion (only observed in chalcogenides). In KFeAs only one hole pocket(s) is present at  $\Gamma$  and is predicted to have  $d$ -wave pairing.[19] On the contrary, in iron-selenide only one (or two concentric) electron-pocket(s) appeared at  $(\pi, 0)/(0, \pi)$ . [2–5] The role of FS topology and the interplay between electron and hole pockets and exact shape of neutron scattering intensity as a conse-

quence of change in FS shape changes across these compounds remains a major question in the field. In this paper we investigate the unusually located electron pockets in iron-selenide superconductors and their role in magnetic susceptibility that we find to have significant stripe like pattern; we also find that thus found spin susceptibility leads to  $d_{x^2-y^2}$ -wave pairing and a spin resonance peak at  $Q$  with ‘hour-glass’ dispersion in the SC state.

We use an effective two band model consisting of strongly hybridized  $t_{2g}$  orbitals,[20] in TB parametrization of the LDA dispersion.[5] We find that the strong instability in the static susceptibility is evolved around an incommensurate vector  $q = (\pi, 0.5\pi)$  at some critical value of  $U$  leading to stripe like SDW or AFM order in these systems, in agreement with experiments.[7–11] Unlike the stripe order in cuprates or other iron based superconductors, here the stripe SDW order have the same  $q$ -modulation at which a  $d_{x^2-y^2}$ -pairing symmetry will possess sign change at the hot-spots.

We show that a magnetic resonance is possible at an slightly incommensurate vector in the case of  $d_{x^2-y^2}$  for the relevant FS shape. Focusing mainly at one doping of  $\text{Tl}_{0.63}\text{K}_{0.37}\text{Fe}_{1.78}\text{Se}_2$ , and at the experimental SC gap value of 8.5meV,[3] we predict the resonance peak to be present in the range of 12.4meV at  $Q = 0.78(\pi, \pi)$ . The resonance profile also yields a ‘hour-glass’ dispersion and 45° rotation of the resonance profile, in close agreement with observations in chalcogenides[16, 17] and cuprates[12] Both the resonance energy and its intensity scales linearly with SC gap amplitude  $\Delta$  and the  $T$ -dependence of the resonance energy and its intensity follows nicely with BCS form of  $\Delta(T)$ , vanishing at  $T_c$ . [14, 18] *TB formalism*: First principle calculations show that the main contribution to the density of states (DOS) near  $E_F$  comes from  $t_{2g}$ -orbitals of Fe 3d states

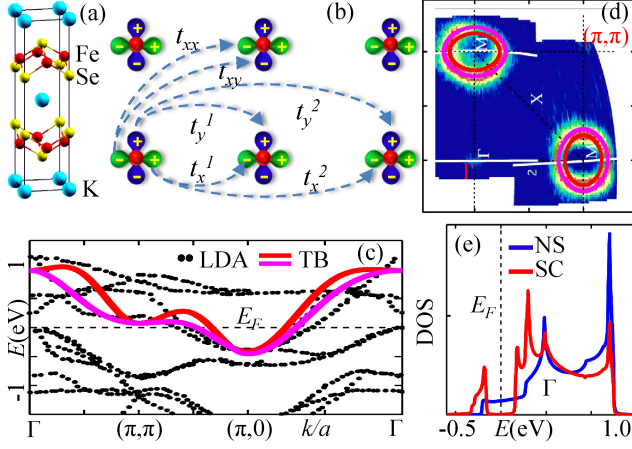


FIG. 1: (Color online) (a) Unit cell of  $\text{KFe}_2\text{Se}_2$ -layered compound. (b)  $x-y$  plane of the unfolded zone with Fe  $3d_{xz}$  and  $3d_{yz}$  orbitals is shown. The arrows depicts various hoppings considered in the present calculation. (c) The resulting two bands are plotted along high-symmetry momenta direction and compared with LDA calculation (black dots).[5] We mainly concentrate on fitting the low-energy part of the band to get the FS shape and their orbital characters in agreement with ARPES. (d) Computed electron pocket FSs overlaid on ARPES data[3]. (e) Normal state (NS) DOS is compared with its SC state result. An artificially large value of SC gap=100meV is chosen to highlight the nodeless and isotropic nature of gap opening at  $E_F$ , despite  $d$ -wave pairing.

which disperse only weakly in the  $z$ -direction.[5] Similar to pnictide[20, 21], the role of the  $d_{xy}$  orbit can be approximated by a next near neighbor hybridization between  $d_{xz}$ ,  $d_{zy}$  orbitals, and we consider a two-dimensional square lattice with two degenerate  $d_{xz}$ ,  $d_{zy}$  orbitals per site. Based on these observations, our model Hamiltonian[20] is

$$H_0 = \sum_{\mathbf{k}, \sigma} \psi_{\mathbf{k}, \sigma}^\dagger [\xi_{\mathbf{k}}^+ \mathbf{1} + \xi_{\mathbf{k}}^- \tau_3 + \xi_{\mathbf{k}}^{xy} \tau_1] \psi_{\mathbf{k}, \sigma}, \quad (1)$$

where  $\sigma$  is the spin index,  $\tau_s$  are Pauli matrices and  $\psi_{\mathbf{k}, \sigma}^\dagger = [d_{xz\sigma}^\dagger, d_{yz\sigma}^\dagger]$  is the two component field operator. We consider up to third nearest-neighbor hopping for the present case as depicted in Fig. 1(b) which gives  $\xi_{\mathbf{k}}^\pm = -(t_x^1 \pm t_y^1)(c_x \pm c_y) - 2(t_{xx} \pm t_{yy})c_x c_y - (t_x^2 \pm t_y^2)(c_{2x} \pm c_{2y}) - \mu^\pm$  and  $\xi_{\mathbf{k}}^{xy} = -4t_{xy}s_x s_y$ . Here  $c/s_i\alpha = \cos/\sin(ik_\alpha a)$  for  $\alpha = x, y$ .  $\mu^+ = \mu$  and  $\mu^- = 0$ .

Hamiltonian in Eq. 1 can be diagonalized straightforwardly obtaining the eigenstates  $E_{0\mathbf{k}}^\pm = \xi_{\mathbf{k}}^+ \pm \xi_{\mathbf{k}}^0$ , where  $\xi_{\mathbf{k}}^0 = \sqrt{(\xi_{\mathbf{k}}^-)^2 + (\xi_{\mathbf{k}}^{xy})^2}$ . [20] The TB parameters are obtained after fitting the dispersion to the LDA calculations,[5] Fig. 1(c):  $(t_x^1, t_y^1, t_{xx}, t_{yy}, t_x^2, t_y^2, t_{xy}) = (-0.12, -0.108, -0.12, -0.12, 0.048, 0.108, 0.06)\text{eV}$  and  $\mu = -0.36\text{eV}$ . To obtain the experimental FS, we use rigid band shift to  $\mu = -0.56\text{eV}$  and get two concentric squarish electron pockets centering  $(\pi, 0)$ , in

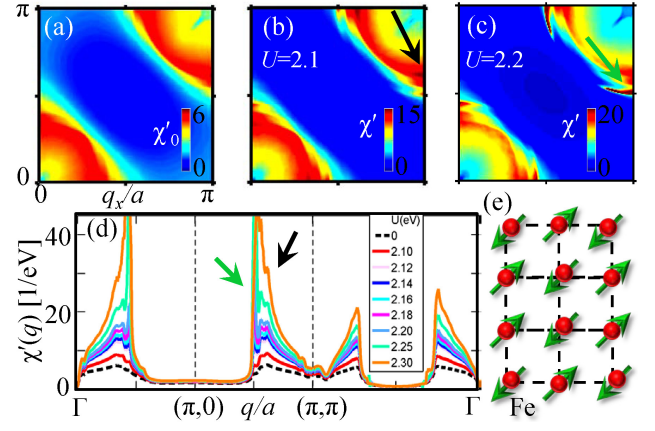


FIG. 2: (Color online) Bare static  $\chi'_0(q) = \sum_{ijkl} \chi'_{ijkl}(q, \omega = 0)$  ( $i, j, k, l$  are orbital indices[22]) is shown in (a) and its RPA part,  $\chi'(q)$ , for two representative values of  $U$  are shown in (b) and (c). (d) The evolution of same  $\chi'(q)$  for different values of  $U$  is drawn along the high-symmetry lines. The black and green arrows separate the peaks in  $\chi'(q)$  coming from the inner and outer FS pockets (see text). (e) Schematic top view of the FeSe layer with the Fe spins in the stripe AFM order expected in our calculation are shown by the arrows.

good agreement with ARPES[3] shown in color plot in Fig. 1(d).

As shown below, for such FS nesting along  $(\pi, \pi)$  is most pronounced leading to a  $d_{x^2-y^2}$ -pairing symmetry according to conventional views. We include SC gap with same amplitude on each band to obtain the SC quasiparticle dispersion as  $E_{\mathbf{k}}^\pm = \sqrt{(E_{0\mathbf{k}}^\pm)^2 + \Delta_{\mathbf{k}}^2}$  where  $\Delta_{\mathbf{k}} = \Delta_0(\cos k_x a - \cos k_y a)/2$ , for the  $d_{x^2-y^2}$ -gap.  $\Delta_0$  is taken from ARPES to be of 8.5meV,[3] for both eigenstates throughout this paper, except for Fig. 1(e) where an artificially large value of  $\Delta_0$  is chosen to explicate the behavior of unconventional gap opening on the DOS. In spite of the presence of nodes in the underlying gap symmetry, the dispersion at all momenta and the resulting DOS exhibit nodeless behavior in Fig. 1(e) as the FS pieces in these compounds are small in size and reside centering at the four-fold symmetric momenta of the gap maxima, similar to pnictide but unlike in cuprate. The nodeless and isotropic gap is observed in ARPES[2-4] and specific heat measurements[6].

*Static susceptibility:* We now proceed to the spin-susceptibility,  $\chi$ , calculation of our model Hamiltonian in the SC state. The calculation of BCS  $\chi$  for a multi-band system including matrix-element effects of all the orbitals is standard and can be found for example in Refs. 20, 21, 23. We consider the electron-electron correlation on the same Fe atom within RPA formalism.[21] The terms in the RPA interaction vertex  $U_s$  that are included in the present calculation are intraorbital interaction  $U$ , an interorbital interaction  $V$ , Hund's rule coupling  $J > 0$ , and the pair hopping strength  $J'$ . In analogy

to crystal and orbital symmetry of FeAs-compounds, we take  $V = U - 5J/4$ ,  $J = U/4$  and  $J' = J$ . [23]

Due to the specific nature of the FS shown in Fig. 1(d), the interpocket nesting is the dominant and incommensurate centering at  $q = (\pi, \pi)$ , see static bare  $\chi'_0(q)$  in Fig. 2(a). [22] An additional nesting occurs centered at  $q = 0$  due to intrapocket nesting of the semi-squarish portion of the FSs. Note that  $q = 0$  nesting is subject to the accuracy of the band structure calculation and its intensity will diminish when the FSs tend towards circular in shape with doping or for different materials. While the shape of  $\chi'_0(q)$  is governed by the shape of the FS, the corresponding intensity is related to the Fermi velocity of the corresponding ‘hot-spots’. [24] Each of the  $\chi'_0(q)$  pattern is split into two due to the splitting of the electron pockets into two concentric ones for our choice band parameters and chemical potential.

Within RPA, at different critical values of  $U$ , one or the other piece of  $\chi'(q)$  will dominate, leading to SDW order phase, see Fig. 2(b-e). To clarify that, we study the evolution of the RPA susceptibility at different values of  $U$ , keeping the other interactions same with respect to the value of  $U$  (following the expressions given above). For a broad range of  $U$  studied in this case, the incommensurate peak around  $q = (\pi, \pi)$  is the winner, suggesting that a stripe like SDW order will be present in this class of materials. These observations are consistent with LDA calculations [5] as well as with number of experiments. [7–11] In the small range of  $U$ , the inner electron pocket gains more intensity (as in the case of  $\chi_0$ , indicated by black arrows), while the outer one is comparatively small (green arrows). Interestingly, when  $U > 2.2\text{eV}$ , the situation is dramatically reversed and the outer nesting develops remarkable instability properties both around  $q = (\pi, \pi)$  and  $q = 0$ , although the former is always dominant in the range of  $U$  studied here. With careful observation, one can find that the strong intensity within RPA is shifted toward  $q = (\pi, 0.5\pi)/(0.5\pi, \pi)$ . This specific incommensurate vector is responsible for the possible  $45^\circ$  rotation of the dynamical magnetic resonance spectra below the resonance energy at some critical value of  $U$  as calculated below, which is remarkably similar to the case of cuprate.

The small  $q = (0, 0.46\pi)/(0.46\pi, 0)$  nesting which we find to be considerably large for our choice of parameters is close to the  $q = 0$  ferromagnetic (FM) instability or may induce some form of charge-density wave (CDW) with finite  $q$  modulation. Note that the coexistence of CDW and SDW due to multiple nestings is an emergent phenomena predicted in pnictide [25] and cuprates [24]. Scanning tunneling microscopy (STM) may be able to detect it.

*Superconductivity:* Unlike the  $(\pi, 0)$ –CDW order in cuprates or  $(\pi, 0)$ –SDW order in pnictide, here the  $q = (\pi, 0.5\pi)/(0.5\pi, \pi)$ –stripe SDW order will facilitate  $d_{x^2-y^2}$ –pairing symmetry. This is due to the fact the

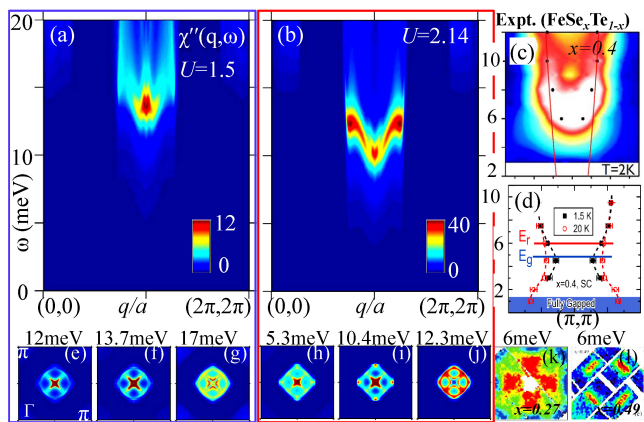


FIG. 3: (Color online) Computed BCS-RPA  $\chi''(q, \omega)$  for  $U = 1.5\text{eV}$  and  $U = 2.14\text{eV}$  are shown in (a) and (b) respectively. The constant energy spectra at three representative energies in the lower panel of the corresponding spectra. The right-hand column shows the neutron data of  $\text{FeTe}_{1-x}\text{Se}_x$ , demonstrating the observations of upward dispersion [15] in (c), ‘hour-glass’ pattern [16] in (d), and  $45^\circ$  rotation of the spectra [17] in (k-l) in this compound.

$q = (\pi, 0.5\pi)/(0.5\pi, \pi)$ –nesting comes from the inter-electron pockets at which the  $d_{x^2-y^2}$ –pairing order possess change in sign of the gap, which is the criterion for the spin resonance to occur as calculated below. But  $q = (0, 0.46\pi)/(0.46\pi, 0)$  instability will provide pair-breaking contributions to the  $d_{x^2-y^2}$ –symmetry.

Based on these findings, we proceed to study the evolution of the spin resonance spectra in the SC state, i.e.,  $\chi''(\mathbf{q}, \omega)$  (RPA-BCS) which is directly measured by Neutron scattering experiment. In the SC state,  $\chi'_0(\mathbf{q}, \omega)$  is strongly enhanced for  $\omega < 2\Delta$  due to turning on of the pair-scattering terms in it. This reduces the critical value of the interaction  $U$  to satisfy the RPA denominator to be positive at  $U\chi'_0(\mathbf{q}, \omega) \leq 1$ . We show the resonance spectra for  $U = 1.5\text{eV}$  in Fig. 3(a) and  $U = 2.14\text{eV}$  in Fig. 3(b) which obtain a commensurate and an incommensurate resonance respectively in addition to their characteristic dispersion.

The dispersion of  $\chi''(\mathbf{q}, \omega)$  which has one-to-one correspondence to the dispersion of  $\chi'_0(\mathbf{q}, \omega)$ , comes from three conditions [21, 23, 26] in addition the matrix-element effects: (1)  $\omega_{res}(\mathbf{q}) = \sum_{k_F^\nu, k_F^{\nu'}} |\Delta_{\mathbf{k}_F^\nu}| + |\Delta_{\mathbf{k}_F^{\nu'}}|$ , (2)  $\text{sgn}(\Delta_{\mathbf{k}_F^\nu}) \neq \text{sgn}(\Delta_{\mathbf{k}_F^{\nu'}})$ , and (3)  $\mathbf{q} = \mathbf{k}_F^\nu + \mathbf{k}_F^{\nu'}$  where  $\nu, \nu'$  are the band indices. Condition (1) comes from the energy conservation of inelastic scattering of Bogoliubov quasiparticles while (2) constitutes the coherence factors of BCS susceptibility to possess non-zero value. As both FS pockets have same gap symmetries and amplitudes and particularly for FeSe systems where all the FS pockets have isotropic gaps at all  $\mathbf{k}_F$ s, conditions (1) and (2) are satisfied equally at all  $k_{FS}$  for inter electron pocket scatterings with  $d_{x^2-y^2}$ –symmetry. No intensity modu-

lation in  $\chi_0(q)$  is governed by conditions (1) and (2) and the only source of intensity variation is the interplay between the orbital matrix-element effect and condition (3), the latter is simply related to the number of degenerate  $\mathbf{k}_{FS}$ . This means, the upward dispersion of the resonance behavior in FeSe can not be understood by tracking how the gap varies on the FS as happened in cuprates[26], but only from the FS nesting and the matrix-element in the tensor form of  $\chi_0$  and also on the interaction vertex  $U_s$ . [21]

Furthermore, unlike in cuprates where the ‘hour-glass’ dispersion extends to  $\omega = 0$  due to the presence of nodal quasiparticles on the FS, in nodeless FS of FeSe-compounds the spin resonance behavior spans only within  $\Delta$  to  $2\Delta$ . For  $U = 1.5\text{eV}$ , the maximum intensity lies at the bottom of the spectra at the commensurate vector at  $\omega_{res} = 13.5\text{meV}$  with  $\omega_{res}/2\Delta = 0.79$ . Again,  $U = 2.14\text{eV}$ , the maximum intensity shifts to the top of the spectra at an incommensurate vector  $q = 0.78(\pi, \pi)$  at  $\omega_{res} = 12.4\text{meV}$  with  $\omega_{res}/2\Delta = 0.73$ , slightly larger than its average value of 0.64 found in all other unconventional superconductors.[27] The upward dispersion of the magnetic spectra is qualitatively analogous to the one observed by Neutron in  $\text{FeTe}_{0.6}\text{Se}_{0.4}$  superconductors[15] shown in Fig. 3(c), while pnictide superconductors show more commensurate spin resonance within the experimental resolution.[14] By including the weak-intensity of the dispersion below the  $(\pi, \pi)$ -resonance, one can draw an ‘hour-glass’ feature, also seen in chalcogenides[16] in Fig. 3(d)

The constant energy profile of the resonance spectra is more interesting and bears important physical insights. At  $\omega \geq \omega_{res}$  for both values of  $U$ , the resonance profile is squarish with maximum intensity lying along the diagonal and finite intensity along the (100) direction, see Figs. 3(g) and (j). For  $U = 1.5\text{eV}$ , the intensity remains concentrated at  $(\pi, \pi)$  even when  $\omega \leq \omega_{res}$ . Interestingly, for  $U = 2.14\text{eV}$  at  $\omega \leq \omega_{res}$  the peak along the diagonal sharply loses intensity while the intensity peak along the bond direction remains almost same. As a result, the resonance profile is rotated by  $45^\circ$  as one goes down below the resonance. The  $45^\circ$  rotation of the resonance spectra is observed earlier in hole doped cuprates[12] and can also be seen in chalcogenides between two different dopings in the SC state[17] in Fig. 3(k-l).

In pnictide and chalcogenide superconductors but not in cuprates, the  $T$  evolution of the spin resonance follows nicely the BCS mean-field behavior of the SC gap  $\Delta(T)$ . [14, 18] We predict that the similar phenomenon also occurs in FeSe-superconductors. To see that we calculate the  $\Delta(T)$  for multiband system solving standard BCS gap equation with phenomenological pairing strength parameters  $V_{1,2} = 52, 46\text{meV}$  (neglecting interband pairing). The parameters are adjusted to obtain experimental gap of  $\Delta_0 = 8.5\text{meV}$  with BCS ratio  $2\Delta/k_B T_c = 6.7$ , in close agreement with the experimental

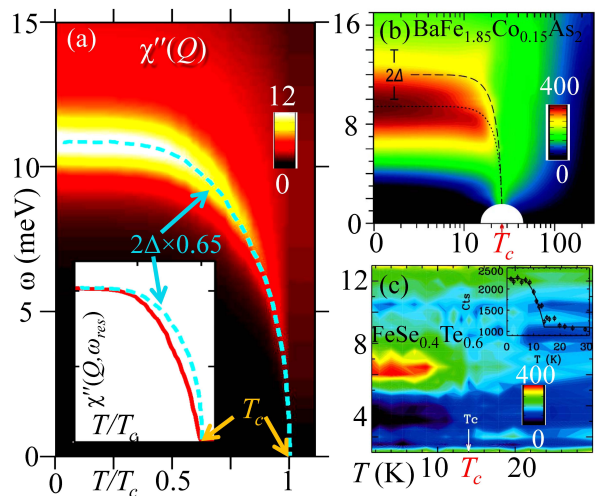


FIG. 4: (Color online)  $T$ -dependence of the spin excitation spectra at  $q = (\pi, \pi)$  for  $U = 1.5\text{eV}$  in (a) is compared with similar result as measured by neutron in pnictide[14] in (b) and in chalcogenides[18] in (c). *inset*: Computed value of the intensity of the resonance peak is compared with BCS  $\Delta(T)$ .

value of 7.[3]  $\Delta(T)$  is shown in Fig 4(a) (cyan line) on top of the calculated RPA-BCS spin resonance spectra at  $q = (\pi, \pi)$  with  $U = 1.5\text{eV}$ . The intensity at the resonance is plotted in *inset* to Fig. 4(a) in red line. Both the resonance energy and the intensity shows a remarkable one-to-one correspondence to  $\Delta(T)$ . The results agree well with pnictide and chalcogenide shown in Fig. 4(b,c) respectively.

In summary, we have calculated the static and dynamical spin susceptibility for an effective two orbitals TB model with  $d_{x^2-y^2}$ -superconductivity. We find that the leading instability in the static susceptibility is evolved around an incommensurate vector  $q = (\pi, 0.5\pi)$  at some critical value of  $U$ , pinning stripe like SDW or AFM order in these systems, in agreement with number of experiments.[7–11] Unlike in other iron based superconductors, here the SDW order have the same  $q$ -vector for the  $d_{x^2-y^2}$ -pairing symmetry to obtain opposite sign at the ‘hot-spot’. Our choice of parameters also predict a comparatively weak CDW modulation with  $q = (0, 0.46\pi)$ , similar to cuprates, pnictides.[24, 25] The  $d$ -wave gap yields a spin resonance behavior with ‘hour-glass’ dispersion and the  $45^\circ$  rotation of the resonance profile, in close agreement with observations in chalcogenides. The  $T$ -dependence of the resonance energy and its intensity follows nicely with BCS form of  $\Delta(T)$ , demonstrating that itinerant RPA-BCS Fermi-liquid theory will be valid in FeSe-based superconductors in particular and in all iron based superconductors studied to date in general.

During the final stage of our work we became aware of preprints by Wang *et al.*[29] and T.A. Maier *et al.*[28] which also predicted the  $d$ -wave gap in FeSe based su-

perconductors.

We are grateful to Hong Ding and A. V. Chubukov for useful discussion. This work was funded by US DOE, BES and LDRD and benefited from the allocation of supercomputer time at NERSC.

- 
- [1] J. Guo *et al.*, Phys. Rev. B **82**, 180520(R) (2010); A. Krzton-Maziopa, *et al.*, arXiv:1012.3637; M. Fang, *et al.*, arXiv:1012.5236.
- [2] Y. Zhang *et al.* arXiv:1012.5980.
- [3] X.-P. Wang *et al.* arXiv:1101.4923.
- [4] D. Mou *et al.* arXiv:1101.4556.
- [5] C. Cao and J. Dai, arXiv:1012.5621; X.-W Yan *et al.*, arXiv:1012.5536, arXiv:1012.6015.
- [6] B. Zeng *et al.* arXiv:1101.5117.
- [7] Hi. Kotegawa *et al.*, arXiv:1101.4572.
- [8] A. M. Zhang *et al.*, arXiv:1101.2168.
- [9] Z. Shermadini *et al.*, arXiv: 1101.1873.
- [10] Z. G. Chen *et al.* arXiv:1101.0572.
- [11] J. J. Ying *et al.*, arXiv:1012.5552.
- [12] P. Bourges *et al.*, Science **288**, 1234 (2000).
- [13] C. Stock *et al.*, Phys. Rev. Lett. **100**, 087001 (2008).
- [14] D. S. Inosov *et al.*, Nat. Phys. **6**, 178 (2010).
- [15] D. N. Argyriou *et al.*, Phys. Rev. B **81**, 220503(R) (2010).
- [16] S. Li *et al.*, Phys. Rev. Lett. **105**, 157002 (2010).
- [17] M. D. Lumsden *et al.*, Nat Phys. **6**, 182 (2010).
- [18] Y. Qiu *et al.*, Phys. Rev. Lett. **103**, 067008 (2009).
- [19] R. Thomale *et al.*, arXiv:1101.3593.
- [20] S. Raghu *et al.*, Phys. Rev. B **77** 220503(R) (2008).
- [21] S. Graser *et al.* New J. Phys. **11**, 025016 (2009).
- [22] We find strongest contributions in  $\chi'_0$  from  $i = j = k = l$ , and the second strongest one from  $i = j \neq k = l$  while the rest are negligibly small or negative.
- [23] T. A. Maier *et al.* Phys. Rev. B **79**, 134520 (2009).
- [24] R. S. Markiewicz *et al.*, Phys. Rev. B **81**, 014509 (2010).
- [25] A. V. Balatsky *et al.* Phys. Rev. B **82**, 144522 (2010).
- [26] I. Eremin *et al.* Phys. Rev. Lett. **94**, 147001 (2005).
- [27] G. Yu *et al.* Nat. Phys. **5**, 873 (2009).
- [28] T.A. Maier *et al.* arXiv:1101.4988.
- [29] Fa Wang *et al.* arXiv:1101.4390.